Journal of Applied Physics

RESEARCH ARTICLE | JULY 22 2024

Microstructure and reflectance of porous GaN distributed Bragg reflectors on silicon substrates

S. Ghosh ; M. Sarkar ; M. Frentrup ; M. J. Kappers ; R. A. Oliver

J. Appl. Phys. 136, 043105 (2024)
https://doi.org/10.1063/5.0216672

View Online

Export Citation

05 August 2024 15:06:13

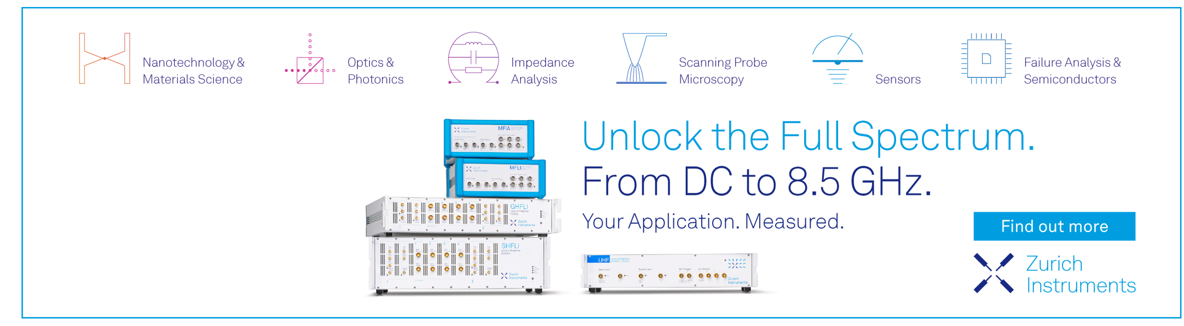

Journal of Applied Physics | ARTICLE | pubs.aip.org/aip/jap

Microstructure and reflectance of porous GaN distributed Bragg reflectors on silicon substrates

Cite as: J. Appl. Phys. **136**, 043105 (2024); doi: 10.1063/5.0216672
Submitted: 30 April 2024 · Accepted: 7 July 2024 ·
Published Online: 22 July 2024

View Online

Export Citation

CrossMark

S. Ghosh, M. Sarkar, M. Frentrup, M. J. Kappers, and R. A. Oliver[a)]

AFFILIATIONS

Department of Materials Science and Metallurgy, University of Cambridge, 27 Charles Babbage Road, Cambridge CB3 0FS, United Kingdom

[a)]**Author to whom correspondence should be addressed:** rao28@cam.ac.uk

ABSTRACT

Distributed Bragg reflectors (DBRs) based on alternating layers of porous and non-porous GaN have previously been fabricated at the wafer-scale in heteroepitaxial GaN layers grown on sapphire substrates. Porosification is achieved via the electrochemical etching of highly Si-doped layers, and the etchant accesses the n^+-GaN layers through nanoscale channels arising at threading dislocations that are ubiquitous in the heteroepitaxial growth process. Here, we show that the same process applies to GaN multilayer structures grown on silicon substrates. The reflectance of the resulting DBRs depends on the voltage at which the porosification process is carried out. Etching at higher voltages yields higher porosities. However, while an increase in porosity is theoretically expected to lead to peak reflectance, in practice, the highest reflectance is achieved at a moderate etching voltage because etching at higher voltages leads to pore formation in the nominally non-porous layers, pore coarsening in the porous layers, and in the worst cases layer collapse. We also find that at the high threading dislocation densities present in these samples, not all dislocations participate in the etching process at low and moderate etching voltages. However, the number of dislocations involved in the process increases with etching voltage.

© 2024 Author(s). All article content, except where otherwise noted, is licensed under a Creative Commons Attribution (CC BY) license (https://creativecommons.org/licenses/by/4.0/). https://doi.org/10.1063/5.0216672

05 August 2024 15:06:13

I. INTRODUCTION

Distributed Bragg reflectors (DBRs) are a key component of numerous optoelectronic devices, including resonant cavity light emitting diodes (RCLEDs),[1] vertical cavity surface emitting lasers (VCSELs),[2] and some designs of single photon source.[3] In the arsenide materials system, the fabrication of such DBRs typically exploits a near-lattice matched pair (lattice mismatch <0.2%) of materials (AlAs and GaAs), which have a significant contrast in refractive index of >0.45. However, in the III-nitride system, the equivalent pair of materials (AlN and GaN) not only have a smaller refractive index contrast (0.15) but also possess a large lattice mismatch of ≈2.4%.[4] In a typical device structure, AlN grows in tension on GaN, and the management of this strain presents a significant challenge.[5,6] An alternative, lattice-matched pair of materials exists, at least for growth in the polar orientation: $Al_{0.82}In_{0.18}N$ and GaN.[4] However, for this pair, the refractive index contrast is even smaller, so that for highly reflective DBRs, a very large number of layers is needed.[4,7] This complexity is costly and inconvenient and imposes limitations on the device design.

Hence, in recent years, the use of porous GaN as an alternative low refractive index material has been explored. This approach was introduced by Zhang *et al.*[8] who used electrochemical etching to porosify n^+-GaN layers within an epitaxial multilayer structure in which the highly doped layers alternated with un-doped layers. In the process flow adopted by Zhang *et al.*, the etchant (highly concentrated nitric acid) accesses the highly doped layers via trenches that cut through the stack. These trenches are defined lithographically using a reactive ion etching process. The need for the definition and creation of trenches adds expense and complexity to the porosification process. Hence, an alternative approach was developed,[9] in which naturally occurring threading dislocations in a GaN/sapphire epitaxial structure are used as channels to transport the etchant and etch products to and from the n^+-GaN layers, respectively.[10] This approach allows full large-area GaN/sapphire wafers to be etched,[9] leaving the wafer surface suitable for further epitaxy and the overgrowth of device structures.[11]

To the best of our knowledge, the dislocation-mediated approach to the fabrication of porous DBRs has, to date, only been explored in the context of GaN/sapphire epitaxy. However, extending

© Author(s) 2024

this approach to GaN-on-Si has notable advantages. Si substrates are cheap and widely available in large sizes, and GaN growth on Si wafers of up to 300 mm diameter has been industrially demonstrated.[12] Moreover, the GaN-on-Si platform has been shown to be amenable to separation of the GaN epitaxy from the substrate to facilitate heterogeneous integration of nitride devices with other materials via transfer printing[13] and other techniques.[12] Here, we, thus, explore the defect-mediated electrochemical etching of GaN-on-Si, illustrating that the defect-mediated process previously observed in GaN/sapphire is also applicable in this case. Furthermore, we explore the impact of varying etching voltage on the morphology of the porous layers and the reflectance of the resulting DBRs. DBR structures consisting of just five periods of alternating porous and non-porous GaN are addressed here to explore what may be achieved with such a relatively thin epitaxial stack and to allow variations in the reflectance arising from different etching conditions to be explored more easily.

II. METHODS

Nitride epilayer growth was carried out by metalorganic vapor phase epitaxy (MOVPE) in an Aixtron close-coupled showerhead reactor on a (111)-oriented 150 mm Si wafer. The epitaxial structure is illustrated in Fig. 1. Prior to the growth of the epilayer, the wafer was heated to ~1080 °C in a hydrogen (H_2) atmosphere for 30 min to desorb the native oxide layer. A buffer structure was then grown consisting of a 250 nm AlN nucleation layer, a 1700 nm graded AlGaN buffer (from 75 at. % Al to 25 at. % Al), and a 725 nm non-intentionally doped (NID) GaN buffer which, after 140 nm, included a SiN_x interlayer to reduce the threading dislocation density.[14] Onto this buffer, a 200 nm Si-doped (at 5×10^{18} cm^{-3}) GaN layer was grown to provide a conductive pathway beneath the DBR. Next, a 200 nm NID GaN layer was added, followed by five periods of a latent DBR structure, each consisting of 58 nm highly Si-doped (at 1×10^{19} cm^{-3}) GaN and 41 nm NID GaN. Trimethylgallium, trimethylaluminum, ammonia, and silane were used as the Ga, Al, N, and Si sources, respectively. The different conductivities achieved under the relevant growth conditions have previously been confirmed by scanning capacitance microscopy[15] and scanning spreading resistance microscopy.[16] All samples subjected to electrochemical etching in this study are taken from the same GaN-on-silicon wafer and are expected to have very similar dislocation densities, in the low-10^9 cm^{-2} regime. The 150 mm wafer was divided into (1.5×2.5) cm^2 chips for porosification, but no lithographic processing was performed.

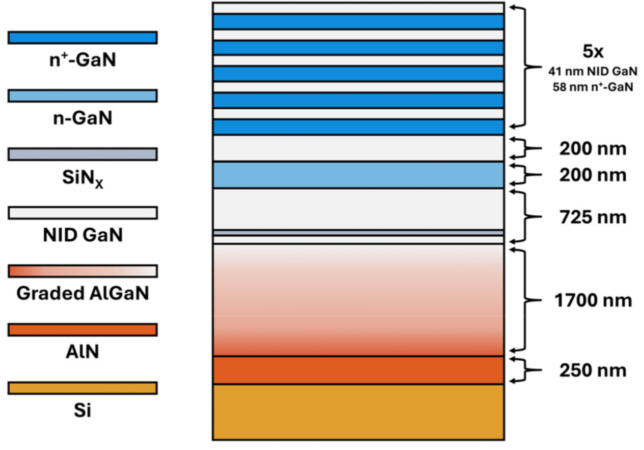

FIG. 1. Simplified schematic of the as-grown epitaxial structure, prior to porosification.

The electrochemical porosification process used to selectively porosify the highly-doped n-type layers is described in detail elsewhere[9] in the context of etching GaN/sapphire DBRs. A 0.25 M solution of oxalic acid was used as the electrolyte, consistent with our previous work on GaN/sapphire,[9] with indium solder used to make ohmic electrical contacts to the sample. A positive bias between 3 and 12 V was applied between the sample and a platinum counter-electrode, injecting holes into the n^+-type layers at the GaN/electrolyte interface. This process is believed to selectively oxidize the gallium, which then dissolves, releasing nitrogen.[17] The etching process was run for 4200 s for each sample, by which time for all samples the etching current had reduced to a characteristic plateau that indicates the completion of the etching process.

The morphologies of the porosified samples were characterized using scanning electron microscopy (SEM) performed in a Zeiss GeminiSEM 300. Plan-view backscattered electron (BSE) imaging was performed on as-porosified samples without sample preparation. High primary electron landing energies (LEs) of 20 keV were used to enable the visualization of sub-surface features. The contrast in such BSE-SEM is dominated by the morphology of the porous layer nearest to the sample surface in a DBR sample.[18] Samples were cleaved to allow cross-sectional imaging, which was carried out using the in-column secondary electron (SE) detector at 2 keV LE. Reflectance spectra were measured using an Accent/Nanometrics RPM 2000 rapid photoluminescence mapper in the normal incidence geometry using a parallel beam from a broadband white light source. To quantify the reflectance, we normalized the reflected signal at the photodetector of our samples with respect to a pre-calibrated commercially available metallic mirror (sourced from Thorlabs). Modeling of reflectance spectra was carried out using a transfer matrix model based on Refs. 19–21 implemented in Microsoft Excel. In our transfer matrix model, we have included the Si substrate (assuming an ordinary refractive index value of 5.0989)[22,23] and the 250 nm AlN nucleation layer (assuming an ordinary refractive index of 2.1889).[23,24] We have treated the graded AlGaN buffer as an AlGaN layer of constant composition with an average refractive index of 2.3407 and have treated all the non-porous GaN layers as having an ordinary refractive index of 2.5263.[23,25] For the porous layers, we have assumed that the porosity is the same in all five DBR layers. We have calculated the refractive index as the geometric mean of GaN and air, using porosity values estimated using BSE-SEM. We note that the values of refractive index that we use are relevant at a wavelength of 420 nm. The model does not take into account refractive index variations with wavelength. The model also does not include the impact of absorption or scattering. The thicknesses of the layers in the DBR are assumed to be 58 and 41 nm for the porous and non-porous layers, respectively, as per the original design for the epitaxy.

05 August 2024 15:06:13

© Author(s) 2024

III. RESULTS

In order to address whether similar morphologies arise in GaN-on-Si to those seen for the more widely explored GaN/sapphire case, we first compare high LE BSE-SEM images of one of our DBRs grown on Si and etched at 5 V [Fig. 2(a)], with a previously studied[18] GaN DBR on sapphire etched under similar conditions [Fig. 2(b)]. The images, which are dominated by the structure of the porous layer closest to the surface (as previously noted), show that the two samples have very similar morphologies. In both cases, we see fields of porosity that center on a small black dot. These black dots are also observed in transmission electron microscopy (TEM) imaging of such samples, where they have been identified as threading dislocations whose cores have opened out into nanopipes during the electrochemical etching process.[10] From these black dots, mid-gray pores emanate roughly radially, separated by white regions, which represent unetched GaN. Where fields of porosity meet, unetched boundaries are observed. In both samples, some branching of the pores is observed. The density of black dots in Fig. 2(a) is $\sim 1 \times 10^9\,\text{cm}^{-2}$, as compared to $\sim 7 \times 10^8\,\text{cm}^{-2}$ for the GaN/sapphire sample [Fig. 2(b)]. For the GaN/sapphire sample, this number is consistent with the expected dislocation density in the material, which is in the mid-$10^8\,\text{cm}^{-2}$. For the GaN-on-silicon sample, the dislocation density is expected to be in the low-$10^9\,\text{cm}^{-2}$ regime, since the SiN_x interlayer reduces the dislocation density from the mid-$10^9\,\text{cm}^{-2}$ level observed for standard structures.[26] However, the fairly similar density of nanopipes in both samples suggests that it is worth exploring whether all dislocations have formed nanopipes in the higher dislocation density GaN-on-silicon material. Overall, however, these data suggest that a similar mechanism of sub-surface porosification via threading dislocations operates in both the GaN-on-silicon sample and the GaN/sapphire sample.

Next, we study the reflectances of DBRs etched under different applied voltages from 3 to 12 V. Figure 3(a) shows the white light reflectance curves for the various samples. For all samples except that etched at 12 V, we see a clearly defined stopband centered at around 450 nm. The stopband for the sample etched at 12 V is blueshifted to ∼425 nm and exhibits a significantly lower peak reflectance than all the other samples. We also note that the fringes in the reflectance spectra, which are present for the majority of the samples, are almost absent in the 12 V sample, which indicates some degree of breakdown of the periodic structure at this voltage. To draw out the trends in peak reflectance across the other samples, in Fig. 3(b), we plot the peak reflectance for each sample against the etching voltage. This graph shows an initial increase in peak reflectance as the etching voltage is increased from 3 (72%) to 5 V (86%) and then a gradual decrease in the peak reflectance from 5 to 10 V (78%), followed by a more pronounced drop between 10 and 12 V (68%).

These changes in reflectance with etching bias are likely to be related to the microstructure of the porous layers. Hence, we now explore these aspects using cross-sectional and plan-view SEM. We focus here on the morphologies of samples etched at 3, , 8, and 12 V—being representative of the changes that occur as the peak reflectance first increases and then decreases. Secondary electron images of each of these samples in cross section are shown in Fig. 4.

In Fig. 4(a), we see the sample etched at 3 V. The first three doped layers from the surface down have been porosified and exhibit small pores of fairly uniform size. However, the fourth layer beneath the surface has only been partially porosified, and the fifth layer only shows fairly limited regions of porosification. Where the doped layers have not been porosified, they show up as slightly darker stripes. This dopant contrast[27] shows that the doped layer is present but has not been etched. However, for the samples etched at 5 and 8 V in Figs. 4(b) and 4(c), we see that all five n^+-GaN layers have been porosified. The pores are perhaps more uniform in size in the 5 V sample than in the 8 V sample. Furthermore, very

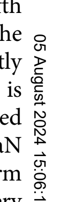
05 August 2024 15:06:13

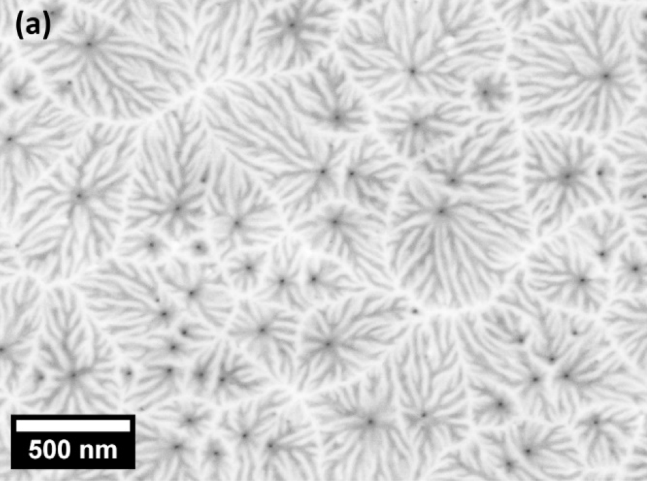

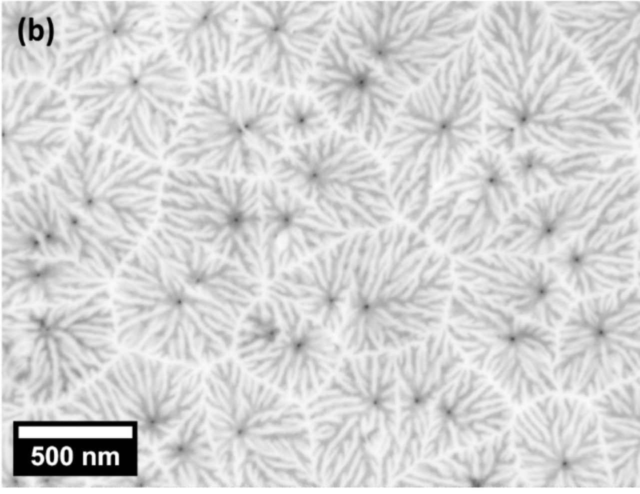

FIG. 2. BSE images showing the morphology of the porous layer nearest to the surface in (a) a GaN-on-Si DBR structure etched at 5 V and (b) a GaN/sapphire DBR structure, etched under similar conditions.

© Author(s) 2024

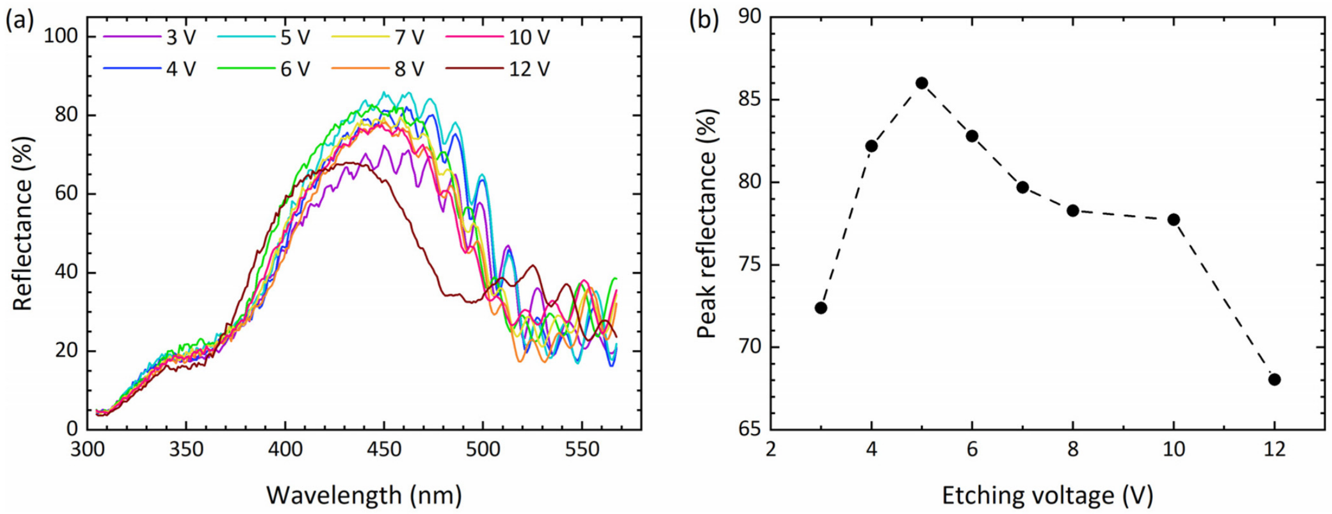

FIG. 3. (a) White light reflectance spectra for samples etched at voltages between 3 and 12 V. (b) Peak reflectance values plotted against etching bias.

little penetration of the porosity into the NID layers is visible for etching at 5 V, although this increases slightly at 8 V. For etching at 12 V in Fig. 4(d), we see a significant density of pores in the NID regions. The highly doped layers have certainly all etched, but the pore sizes are very uneven. There are regions that appear to have been fully electropolished, with none of the doped material remaining, but in other regions, nanoscale porosity is visible. The NID layer between the fourth and fifth doped layers from the surface appears to be absent across much of the image; it may have been lost in cleaving rather than during etching. However, elsewhere in the sample, we see regions where undoped layers have broken and collapsed downward into the etched regions (see the supplementary material).

Next, we consider the additional information about the changes in the pore morphology, which can be achieved from plan-view BSE imaging at high primary electron LE. Figure 5(a) shows the morphology of the porous layer nearest to the surface in the sample etched at 3 V. Similar to the data shown in Fig. 2(a) for the sample etched at 5 V, we see black dots with fields of porosity emanating from them, separated by unetched boundaries. The number of black dots $[(7.8 \pm 0.5) \times 10^8\,\text{cm}^{-2}]$ is lower than for the sample etched at 5 V, and it should be noted that not all black dots are found at the center of a field of porosity, so that the density of fields of porosity is even lower than the density of black dots. A wider field-of-view image of that 5 V sample in Fig. 5(b) shows data consistent with what has previously been presented in Fig. 1(a), with a black dot density of $(11.0 \pm 0.3) \times 10^8\,\text{cm}^{-2}$. However, for the sample etched at 8 V [shown in Fig. 5(c)], we see a substantially higher density of black dots $[\sim(22 \pm 1) \times 10^8\,\text{cm}^{-2}]$. Here, these black dots often appear in lines, consistent with the expected appearance of arrays of edge-type threading dislocations in GaN epitaxial layers.[28] Particularly where pores emanate from such arrays, but also elsewhere, the pores seen here are larger, and no longer exhibit a branched structure. However, between these larger pores, regions of fine porosity persist. This finding echoes the suggestion made based on the cross-sectional data that the 8 V sample showed less uniform pore sizes. At an etching voltage of 12 V, shown in Fig. 5(d), the black dots associated with threading dislocations are clearly larger than for the other samples and might be better described as non-uniform dark gray splotches. These splotches are approximately 70 nm across, in comparison with the more defined black dots seen at lower voltages, whereas the diameters of the black dots are roughly 5, 8, and 14 nm for etching voltages of 3, 5, and 8 V, respectively. They also have a slightly higher density again: $[\sim(25 \pm 2) \times 10^8\,\text{cm}^{-2}]$. The large size and non-uniform shape of the black dots can be related to the etching of the NID layers observed in cross section, which we have suggested elsewhere[18] occurs at dislocation sites. In the plan-view image, we see very large pores of irregular size and shape with occasional fine strands of unetched GaN between them, and very occasional regions of fine-scale porosity.

The observed increase with etching voltage in the density of the black dots associated with nanopipes at dislocation cores suggests that for samples with a high threading dislocation density, the number of threading dislocations actively involved in the etching process is controlled not by the dislocation density but by the etching voltage. For GaN/sapphire samples with a lower dislocation density, we have previously suggested that all the dislocations are actively involved in the etching process.[10] For GaN-on-silicon samples with a higher dislocation density, the data we present in Fig. 5 suggest this is not the case, particularly at low etching voltages. Nonetheless, the overall morphologies we report here are consistent with morphologies we have previously reported at lower and higher etching voltages for GaN/sapphire.[18] We note that our previous studies suggesting that all dislocations are involved in the etching process in GaN/sapphire use etching voltages greater than 5 V and do not address whether either lower etching voltages or

05 August 2024 15:06:13

© Author(s) 2024

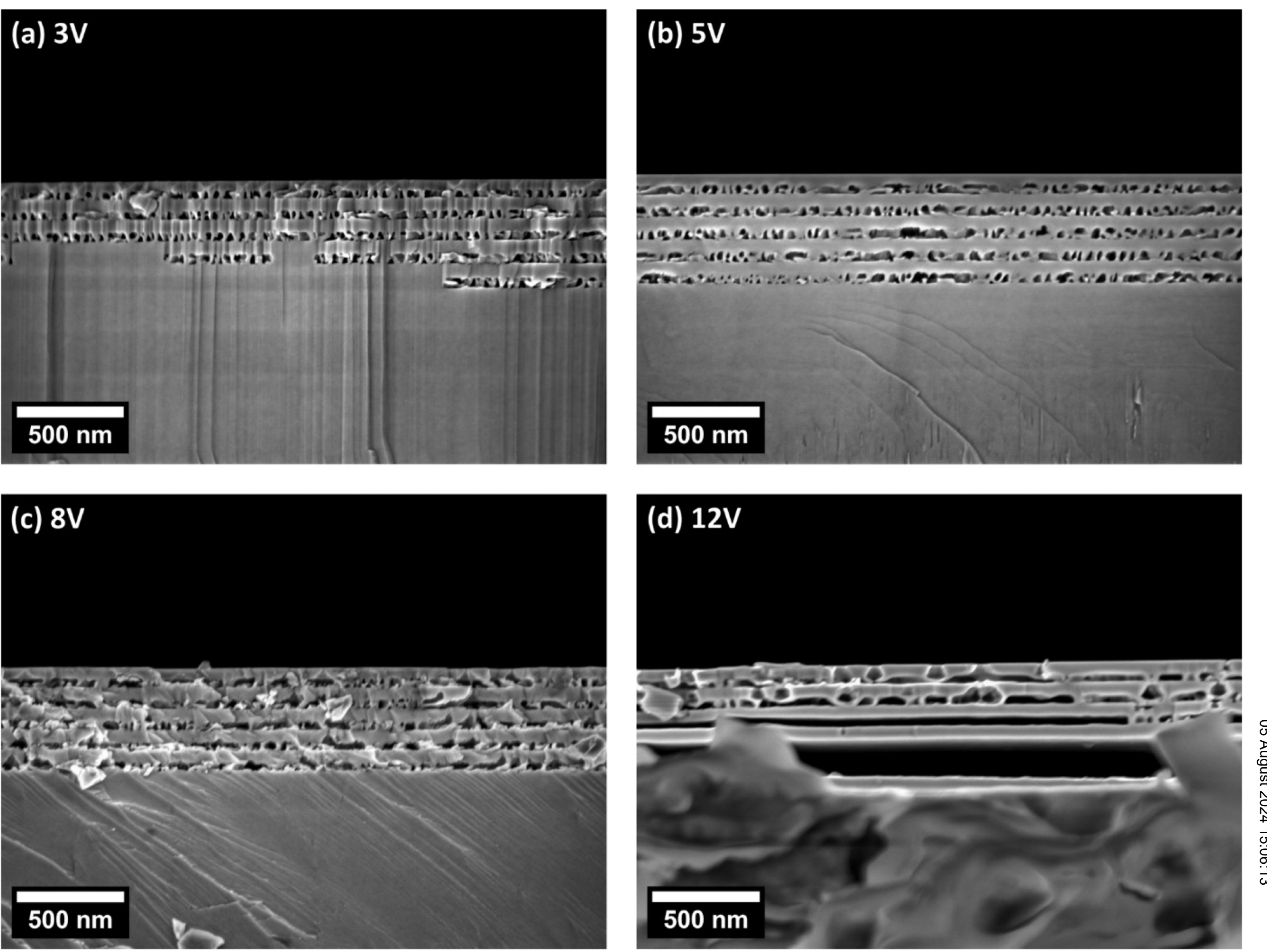

FIG. 4. Representative SE images of cleaved cross sections of GaN-on-silicon DBRs etched at (a) 3, (b) 5, (c) 8, and (d) 12 V.

05 August 2024 15:06:13

higher dislocation densities in GaN/sapphire will also yield a disparity between the dislocation density and the number of dislocations actively involved in etching.

We now address the variation in the porosity with etching voltage more quantitatively, applying a quantitative definition of porosity as the proportion of the doped material that has been removed during the etching process. Porosity quantification was performed based on the data in Fig. 5; i.e., the porosities given here are for the porous layer nearest to the surface. Otsu's intensity thresholding algorithm—implemented within ORS Dragonfly (Object Research Systems, Montreal, Canada)—was used to segment these 8-bit, grayscale BSE images into porous and non-porous material classes.[29] Figure 6 shows the variation in the porosity with etching voltage for the four samples shown in Fig. 5. Each error bar is derived from the standard error over four porosity measurements. As can be seen in the BSE images, the porosity increases significantly with the etching voltage. These findings are qualitatively consistent with the phase diagram of anodic etching reported by Zhang *et al.*[30] They showed that for etching in nitric acid, both porosity and pore size generally increased as the etch voltage increased for a fixed dopant density and etching concentration. However, they saw complete etching of their DBR structures via lithographically defined trenches for etch voltages as low as 1 V. For our samples, etched via dislocation pipelines, a higher etch voltage is required, suggesting that some voltage may be dropped across the narrow channels through the undoped layers.

IV. DISCUSSION

In this discussion, we will address the observed variations in porosity and reflectance with etching voltage, and how and why the observed reflectance deviates from that predicted by a transfer

© Author(s) 2024

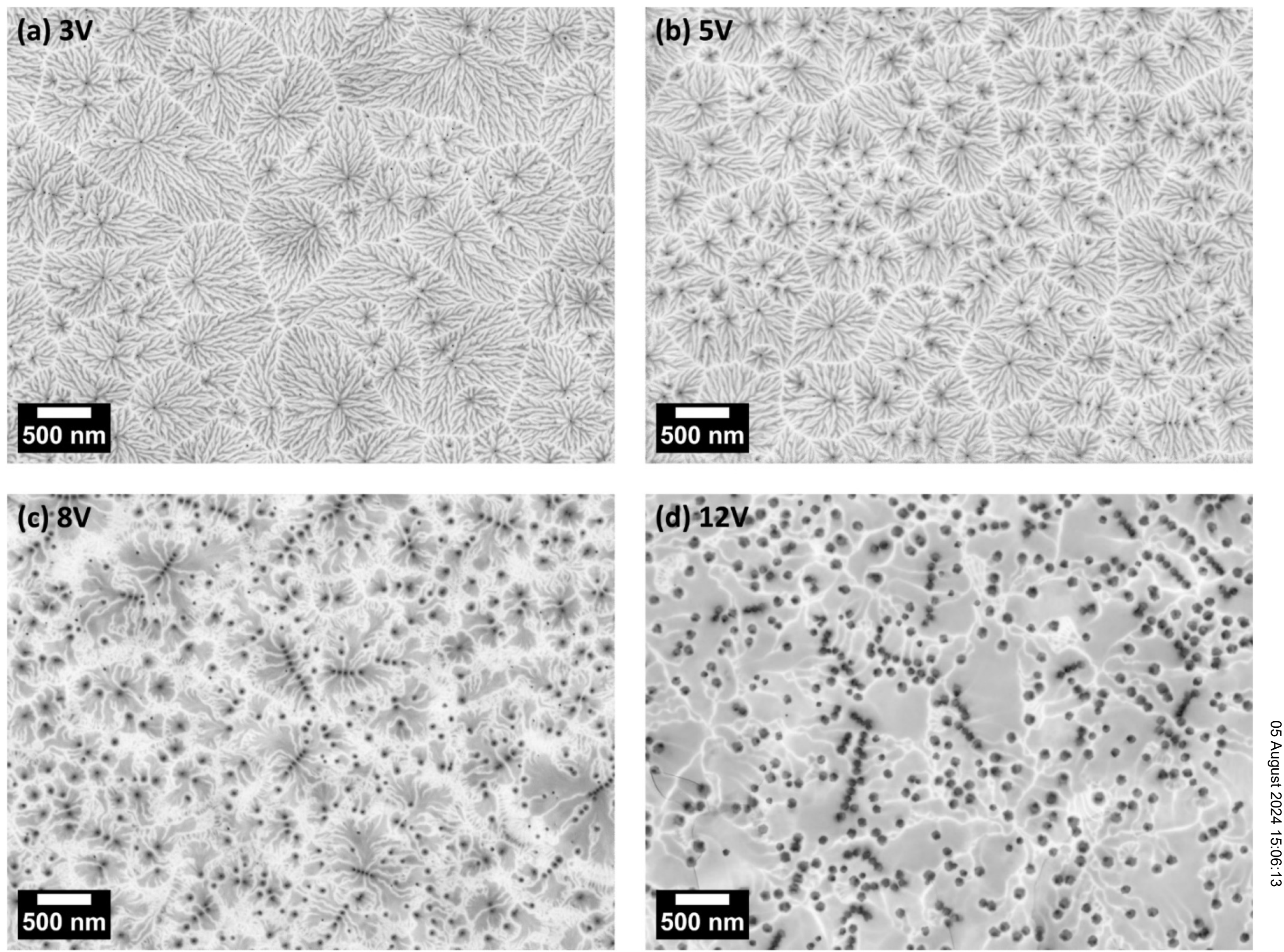

FIG. 5. BSE images showing the morphology of the porous layer nearest to the surface in GaN-on-silicon DBRs etched at (a) 3, (b) 5, (c) 8, and (d) 12 V.

05 August 2024 15:06:13

matrix model (TMM) that calculates the reflectance of a quarter wave stack DBR on a non-native substrate.[19–21]

Figure 7 shows that within the theoretical model, the observed increase in the porosity with applied voltage is expected to lead to a continuous blueshift of the position of the peak (a) and a monotonic increase in the peak reflectance (b). Braniste *et al.* have previously reported similar findings using a TM model.[31] The increase in the peak reflectance occurs despite the fact that these DBRs deviate from the usual design parameters. In general, DBR layer thicknesses are designed for a desired wavelength and their thicknesses are set to be one quarter of the wavelength of light in the material making up the layer. Since the porosity and, thus, the refractive index varies between samples, but the layer thickness is not adjusted to match the change in the porosity, all these DBRs deviate from an "ideal" design. Nonetheless, the model suggests that a very high reflectance—of up to 99.8% for porous layers with 88.4% porosity—should be achievable, even with only five pairs in the DBR. We also note that simulated DBR reflectance for different porosities of the low refractive index layers with the commercially available COMSOL Multiphysics® software showed close agreement with the results of the TM model described above (see the supplementary material). However, referring back to Fig. 3, the reflectance values observed, particularly at the higher voltages, fall far short of the theoretical predictions. (For the reader's convenience, we include in the supplementary material plots where each experimental dataset is compared individually with its corresponding TMM.) For wavelengths shorter than 365 nm, i.e., above the GaN bandgap—the fact that we have ignored absorption in the model will have a substantial impact. Hence, the remainder of this discussion focuses on sub-bandgap reflectance.

The reason that the DBR etched at 3 V has a lower reflectance than predicted is evident from the cross-sectional SEM data: in

© Author(s) 2024

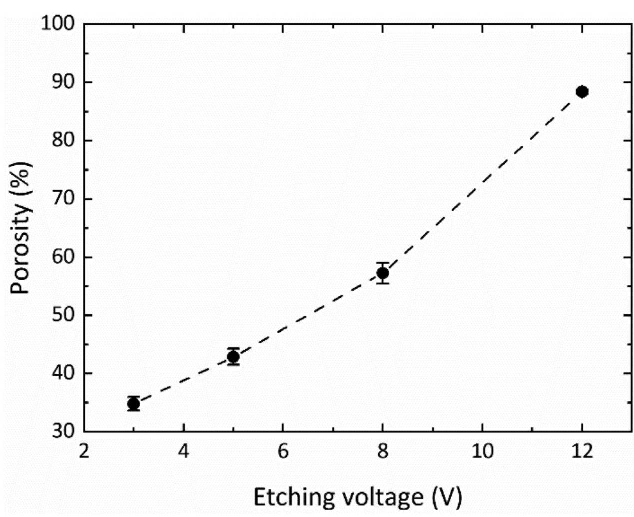

FIG. 6. Variation in the porosity of the layer nearest to the surface with etching bias.

places only the top three highly doped layers have been etched. Using our TMM for a three-pair DBR, we predict a reflectance of ~80%, close to the observed value. In the experimental data, the peak reflectance is achieved at 5 V, under which condition all the doped layers in the DBR have etched. This is obviously a basic prerequisite for achieving a high reflectance.

For etching voltages above 5 V, the SEM data also provide indications as to why the reflectance falls short of the predicted values. Our model assumes that the NID regions remain entirely non-porous. However, above 5 V, increasing porosity is observed in these non-porous layers by cross-sectional SEM, and for the highest etching voltage, this can be correlated to substantial broadening of the dislocation channels that facilitate the etching. This non-intentional porosification may suggest a limitation of the dislocation-mediated etching approach at higher etching voltages. Another issue with the sample etched at 12 V (highlighted in the cross-sectional SEM images) is that layers may collapse or NID GaN layers may be entirely absent. As the etching approaches the electropolishing regime, the periodic structure starts to break down entirely, and hence, reflectance is lowered. From the plan-view images, we also note that the pores are larger and less uniform at the higher applied voltages. An assumption in the application of porous GaN is that the pores are smaller than the wavelength of light. Therefore, the porous materials act as a continuous effective medium whose refractive index is dependent on the porosity. Where the pores are larger, this assumption breaks down, and we may expect to see substantial diffuse light scattering.[32] All the models show more pronounced reflectance fringes than the experimental data, and this may in part be linked to our treatment of the buffer layer in the model, which we comment on further below. However, in the experimental data for the sample etched at 12 V, the fringes are almost entirely absent across the stop band, and this may be due to the impact of scattering. This scattering cannot be modeled using a basic TMM, but we plan to investigate this issue further in future using finite element modeling.

Last, we note that although the highest measured peak reflectance is achieved at 5 V, the experimental value of 86% is slightly less than would be predicted given the experimentally determined porosity of this sample. This predicted value is ≈93%. There are several possible reasons for this. First, there are limitations to the accuracy of our predictions. We may have slightly overestimated the porosity, as porosity measurement methods for porous nitride

05 August 2024 15:06:13

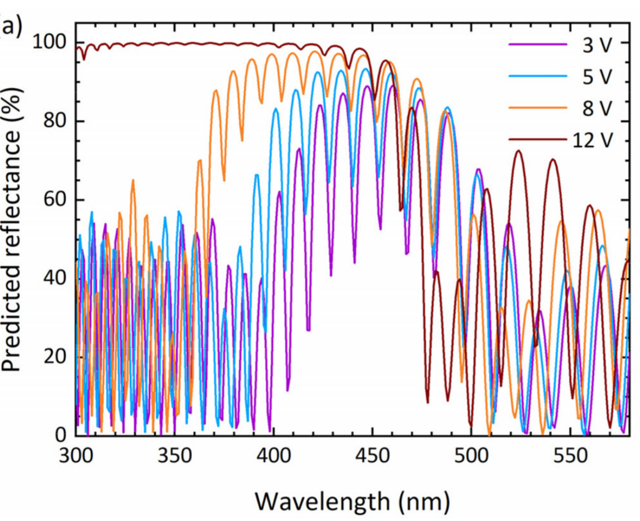

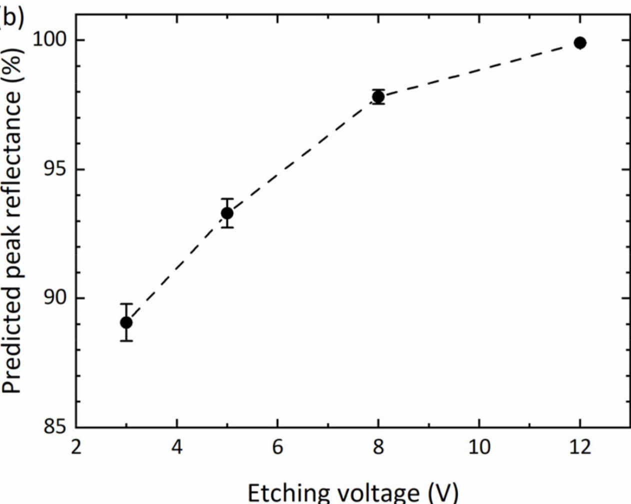

FIG. 7. (a) Predicted reflectance spectra for samples etched at between 3 and 12 V, based on the porosity data in Fig. 6. (b) Predicted peak reflectance values based on the porosity data in Fig. 6 plotted against etching bias.

© Author(s) 2024

DBRs are not well established.[33] Here, we used the plan-view BSE images for porosity estimation since they sample a relatively large area and have clear contrast unaffected by sample preparation, but there may, nonetheless, be shortcomings in our method. Equally, we may not have accurately calculated the refractive index from the porosity. There are a number of different models available for refractive index estimation. However, none are well established in the porous nitrides, in which the crystal structure of the underlying GaN is polar and in which the pores are often elongated.[34] Additionally, our model treats the buffer layer as having a single thick layer of AlGaN of constant refractive index rather than a graded layer. Changes to the buffer layer in the simulation can make a 1%–2% difference to the predicted peak reflectance. However, it is also possible that there are shortcomings in the structure of our DBR that have not been considered. We have assumed that the porosity is the same in all the porous layers. While significant through-thickness porosity variations are not evident in the cross-sectional SEM images of the sample etched at 5 V, such images sample a rather limited area of each porous layer. Equally, some scattering may be occurring even for the small pores achieved at these low etching voltages, and again, future finite element modeling with porosity determined from more accurate methods (e.g., 3D tomography) may provide further insights.

V. CONCLUSION

We have demonstrated that the porosification of DBRs via dislocation channels, which was previously demonstrated in GaN/sapphire, is equally applicable to the GaN-on-Si platform. Within the range of conditions used to etch such DBRs in this study, we have shown that a moderate voltage (here 5 V) leads to optimum DBR reflectance (>85%). Such a voltage ensures that all the intended layers within the DBR are etched while avoiding the negative consequences of etching at higher voltages: unintended porosification of the NID layers and formation of large pores, which may lead to scattering and layer collapse. We note that at these voltages, not all the threading dislocations present in the GaN-on-Si epitaxy appear to be active in the etching process. Overall, although further optimization of the process is required, our studies suggest that even with a fairly limited number of pairs, highly reflective DBRs can be realized on the GaN-on-silicon platform, paving the way for low-cost mass-manufacturable photonic components based on porous GaN.

SUPPLEMENTARY MATERIAL

See the supplementary material for (1) additional zoomed-in secondary electron images of the GaN-on-silicon DBR samples described in the article, (2) reflectance spectra of GaN/porous-GaN DBRs simulated with the COMSOL Multiphysics software, and (3) separate plots for each etching voltage in which the experimental data are compared with the relevant TMM.

ACKNOWLEDGMENTS

This research was supported by the EPSRC under Grant Nos. EP/R03480X/1, EP/W03557X/1, EP/X015300/1, EP/N509620/1, and EP/R513180/1. Rachel Oliver would like to acknowledge funding from the Royal Academy of Engineering under the Chairs in Emerging Technologies Scheme, which is sponsored by the Department for Science, Innovation and Technology (DSIT). We thank Clifford McAleese for his work on the transfer matrix model.

AUTHOR DECLARATIONS

Conflict of Interest

The authors have no conflicts to disclose.

Author Contributions

S.G. and M.S. contributed equally to this paper.

S. Ghosh: Conceptualization (lead); Formal analysis (lead); Investigation (lead); Methodology (lead); Visualization (equal); Writing – original draft (equal); Writing – review & editing (equal). **M. Sarkar:** Investigation (equal); Methodology (equal); Visualization (equal); Writing – review & editing (equal). **M. Frentrup:** Formal analysis (equal); Investigation (equal); Methodology (equal); Visualization (lead); Writing – original draft (equal); Writing – review & editing (equal). **M. J. Kappers:** Formal analysis (equal); Investigation (equal); Writing – review & editing (equal). **R. A. Oliver:** Conceptualization (equal); Formal analysis (equal); Funding acquisition (equal); Investigation (equal); Project administration (equal); Supervision (lead); Visualization (equal); Writing – original draft (lead); Writing – review & editing (equal).

DATA AVAILABILITY

The data that support the findings of this study are openly available in the University of Cambridge repository, Ref. 35.

05 August 2024 15:06:13

REFERENCES

[1] C. Zhang, K. Xiong, G. Yuan, and J. Han, "A resonant-cavity blue–violet light-emitting diode with conductive nanoporous distributed Bragg reflector," Phys. Status Solidi A **214**(8), 1600866 (2017).

[2] S.-M. Lee, S.-H. Gong, J.-H. Kang, M. Ebaid, S.-W. Ryu, and Y.-H. Cho, "Optically pumped GaN vertical cavity surface emitting laser with high index-contrast nanoporous distributed Bragg reflector," Opt. Express **23**(9), 11023–11030 (2015).

[3] H. P. Springbett, K. Gao (高亢), J. Jarman, T. Zhu, M. Holmes, Y. Arakawa, and R. A. Oliver, "Improvement of single photon emission from InGaN QDs embedded in porous micropillars," Appl. Phys. Lett. **113**, 101107 (2018).

[4] J.-F. Carlin, C. Zellweger, J. Dorsaz, S. Nicolay, G. Christmann, E. Feltin, R. Butté, and N. Grandjean, "Progresses in III-nitride distributed Bragg reflectors and microcavities using AlInN/GaN materials," Phys. Status Solidi B **242**(11), 2326–2344 (2005).

[5] G. S. Huang, T. C. Lu, H. H. Yao, H. C. Kuo, S. C. Wang, C.-W. Lin, and L. Chang, "Crack-free GaN/AlN distributed Bragg reflectors incorporated with GaN/AlN superlattices grown by metalorganic chemical vapor deposition," Appl. Phys. Lett. **88**, 061904 (2006).

[6] K. Yagi, M. Kaga, K. Yamashita, K. Takeda, M. Iwaya, T. Takeuchi, S. Kamiyama, H. Amano, and I. Akasaki, "Crack-free AlN/GaN distributed Bragg reflectors on AlN templates," Jpn. J. Appl. Phys. **51**, 051001 (2012).

[7] C. Berger, A. Dadgar, J. Bläsing, A. Lesnik, P. Veit, G. Schmidt, T. Hempel, J. Christen, A. Krost, and A. Strittmatter, "Growth of AlInN/GaN distributed Bragg reflectors with improved interface quality," J. Cryst. Growth **414**, 105–109 (2015).

© Author(s) 2024

[8]C. Zhang, S. H. Park, D. Chen, D.-W. Lin, W. Xiong, H.-C. Kuo, C.-F. Lin, H. Cao, and J. Han, "Mesoporous GaN for photonic engineering—Highly reflective GaN mirrors as an example," ACS Photonics **2**(7), 980–986 (2015).
[9]T. Zhu, Y. Liu, T. Ding, W. Y. Fu, J. Jarman, C. X. Ren, R. V. Kumar, and R. A. Oliver, "Wafer-scale fabrication of non-polar mesoporous GaN distributed Bragg reflectors via electrochemical porosification," Sci. Rep. **7**, 45344 (2017).
[10]F. C.-P. Massabuau, P. H. Griffin, H. P. Springbett, Y. Liu, R. V. Kumar, T. Zhu, and R. A. Oliver, "Dislocations as channels for the fabrication of sub-surface porous GaN by electrochemical etching," APL Mater. **8**, 031115 (2020).
[11]J. C. Jarman, T. Zhu, P. H. Griffin, and R. A. Oliver, "Light-output enhancement of InGaN light emitting diodes regrown on nanoporous distributed Bragg reflector substrates," Jpn. J. Appl. Phys. **58**, SCCC14 (2019).
[12]H. W. Then, M. Radosavljevic, K. Jun, P. Koirala, B. Krist, T. Talukdar, N. Thomas, and P. Fischer, "Gallium nitride and silicon transistors on 300 mm silicon wafers enabled by 3-D monolithic heterogeneous integration," IEEE Trans. Electron Devices **67**(12), 5306–5314 (2020).
[13]B. Guilhabert, S. P. Bommer, N. K. Wessling, D. Jevtics, J. A. Smith, Z. Xia, S. Ghosh, M. Kappers, I. M. Watson, R. A. Oliver, M. D. Dawson, and M. J. Strain, "Advanced transfer printing with in-situ optical monitoring for the integration of micron-scale devices," IEEE J. Sel. Top. Quantum Electron. **29**(3), 7900111 (2023).
[14]M. Kappers, M. Moram, Y. Zhang, M. Vickers, Z. Barber, and C. Humphreys, "Interlayer methods for reducing the dislocation density in gallium nitride," Physica B **401–402**, 296–301 (2007).
[15]J. Sumner, R. A. Oliver, M. J. Kappers, and C. J. Humphreys, "Assessment of the performance of scanning capacitance microscopy for n-type gallium nitride," J. Vac. Sci. Technol. B **26**, 611–617 (2008).
[16]J. Sumner, R. A. Oliver, M. J. Kappers, and C. J. Humphreys, "Assessment of scanning spreading resistance microscopy for application to n-type GaN," Phys. Status Solidi C **5**(6), 1652–1654 (2008).
[17]P. H. Griffin and R. A. Oliver, "Porous nitride semiconductors reviewed," J. Phys. D: Appl. Phys. **53**, 383002 (2020).
[18]M. Sarkar, F. Adams, S. A. Dar, J. Penn, Y. Ji, A. Gundimeda, T. Zhu, C. Liu, H. Hirshy, F. C.-P. Massabuau, T. O'Hanlon, M. J. Kappers, S. Ghosh, G. Kusch, and R. A. Oliver, "Sub-surface Imaging of Porous GaN Distributed Bragg Reflectors via Backscattered Electrons," Microsc. Microanal. **30**(2), 208–225 (2024).
[19]E. F. Schubert, J. K. Kim, H. Luo, and J.-Q. Xi, "Solid-state lighting—A benevolent technology," Rep. Prog. Phys. **69**(12), 3069 (2006).
[20]E. F. Schubert and N. E. J. Hunt, "Enhancement of spontaneous emission in microcavities," in *Vertical-Cavity Surface-Emitting Lasers—Design, Fabrication, Characterization, and Applications* (Cambridge University Press, Cambridge, 1999), pp. 68–107.
[21]W. G. Breiland, A. A. Allerman, J. F. Klem, and K. E. Waldrip, "Distributed Bragg reflectors for vertical-cavity surface-emitting lasers," MRS Bull. **27**, 520–524 (2002).
[22]D. E. Aspnes and A. A. Studna, "Dielectric functions and optical parameters of Si, Ge, GaP, GaAs, GaSb, InP, InAs, and InSb from 1.5 to 6.0 eV," Phys. Rev. B **27**, 985 (1983).
[23]M. N. Polyanskiy, "Refractiveindex.info database of optical constants," Sci. Data **11**, 94 (2024).
[24]J. Pastrňák and L. Roskovcová, "Refraction index measurements on AlN single crystals," Phys. Status Solidi B **14**, K5–K8 (1966).
[25]J. A. S. Barker and M. Ilegems, "Infrared lattice vibrations and free-electron dispersion in GaN," Phys. Rev. B **7**, 743 (1973).
[26]S. Ghosh, A. M. Hinz, M. Frentrup, S. Alam, D. J. Wallis, and R. A. Oliver, "Design of step-graded AlGaN buffers for GaN-on-Si heterostructures grown by MOCVD," Semicond. Sci. Technol. **38**, 044001 (2023).
[27]S. Chung, V. Wheeler, R. Myers-Ward, L. O. Nyakiti, C. R. Eddy, D. K. Gaskill, M. Skowronski, and Y. N. Picard, "Secondary electron dopant contrast imaging of compound semiconductor junctions," J. Appl. Phys. **110**, 014902 (2011).
[28]R. Oliver, M. Kappers, J. Sumner, R. Datta, and C. Humphreys, "Highlighting threading dislocations in MOVPE-grown GaN using an *in situ* treatment with SiH4 and NH3," J. Cryst. Growth **289**(2), 506–514 (2006).
[29]N. Otsu, "A threshold selection method from gray-level histograms," IEEE Trans. Syst. Man. Cybern. **9**(1), 62–66 (1979).
[30]C. Zhang, G. Yuan, A. Bruch, K. Xiong, H. X. Tang, and J. Han, "Toward quantitative electrochemical nanomachining of III-nitrides," J. Electrochem. Soc. **165**(10), E513 (2018).
[31]T. Braniste, J. Ciers, E. Monaico, D. Martin, J.-F. Carlin, V. V. Ursaki, V. V. Sergentu, I. M. Tiginyanu, and N. Grandjean, "Multilayer porous structures of HVPE and MOCVD grown GaN for photonic applications," Superlattices Microstruct. **102**, 221–234 (2017).
[32]J. Park, J.-H. Kang, and S.-W. Ryu, "High diffuse reflectivity of nanoporous GaN distributed Bragg reflector formed by electrochemical etching," Appl. Phys. Express **6**, 072201 (2013).
[33]I. S. Isa, S. M. Isa, A. Abd Manaf, A. F. Abd Rahim, A. Mahmood, M. H. Abdullah, and N. Ad Fauzi, "Morphological and structural characteristics of gallium nitride (GaN) porosity using image processing," Optik **271**, 170126 (2022).
[34]P. H. Griffin, K. M. Patel, T. Zhu, R. M. Langford, V. S. Kamboj, D. A. Ritchie, and R. A. Oliver, "The relationship between the three-dimensional structure of porous GaN distributed Bragg reflectors and their birefringence," J. Appl. Phys. **127**(19), 193101 (2020).
[35]S. Ghosh, M. Sarkar, M. Frentrup, M. J. Kappers, and R. A. Oliver, "Research data supporting 'Microstructure and reflectivity of porous GaN distributed Bragg reflectors on silicon substrates'," (2024).

05 August 2024 15:06:13

© Author(s) 2024